Supplementary Table 1 Trend in the global carbon cycle during three time periods: the whole study period, warming period and warming hiatus. We calculate the trends based on linear least square regression analysis. The slope of the regression was then defined as the trend. The standard error of linear regression coefficient (slope) was defined as the uncertainty of the linear trend. Note that for the average trend of different data sources, the uncertainty of its trend was estimated as the root-mean-square of the standard error of for each data sources under the assumption that data from different datasets is independent from each other. The significant trends ($P < 0.05$) based on t test are denoted with two asterisks. Here the DGVMs from the TRENDYv2 project were driven by rising atmospheric CO_2 concentration and climate change.

		Whole study period (1980-2012)	**Warming period (1980-1998)**	**Warming hiatus (1998-2012)**
NLS	MACC	0.088±0.018**	0.077±0.048	0.173±0.047**
	JENA	0.074±0.017**	0.041±0.043	0.155±0.054**
	GCP	0.060±0.020**	0.023±0.054	0.175±0.062**
	mean±1 SE	0.074±0.019**	0.047±0.049**	0.168±0.054**
NPP	SM16	0.051±0.013	0.115±0.027**	0.039±0.041
	DGVMs (mean±1 SE)	0.162±0.018**	0.153±0.041**	0.152±0.059**
HR	DGVMs (mean±1 SE)	0.134±0.013**	0.101±0.032**	0.091±0.033**

Supplementary Table 2 Change in trends of the global net land carbon sink (NLS) and that in carbon emission from land use change (E_{LUC}) during the warming hiatus compared to the warming period. Year of 1997, 1998, 2001 and 2002 was used as the dividing line to separate the warming period and the warming hiatus period, respectively. The statistics of the change in trend of NLS and E_{LUC} were estimated using bootstrap analyses (see Methods). The statistically significant change in trends ($P < 0.05$) are denoted with two asterisks. E_{LUC} was estimated using the bookkeeping methods following Houghton et al. (2017).

Dividing line	Change in NLS trend (NLS intensification) (Pg C yr^{-2})	Change in E_{LUC} trend (Pg C yr^{-2})	Contribution of E_{LUC} to NLS intensification
1997	0.080±0.064	0.113±0.014**	142%
1998	0.124±0.069**	0.088±0.009**	71%
2001	0.118±0.073**	0.074±0.011**	63%
2002	0.159±0.080**	0.077±0.010**	49%

Supplementary Table 3 Details of seven versions of JENA atmospheric CO_2 inversions. The seven versions differ in number of atmospheric sites used in the inversion and the corresponding period of validity.

Version	Atmospheric sites	Period of validity
s81_v3.8	15	1981-2015
s85_v3.8	21	1985-2015
s90_v3.8	27	1990-2015
s93_v3.8	38	1993-2015
s96_v3.8	48	1996-2015
s99_v3.8	55	1999-2015
s04_v3.8	61	2004-2015

Supplementary Table 4 Global and regional forest area in 1990, 2000 and 2010 derived from the Forest Resources Assessment 2015 by Food and Agriculture Organization of the United Nations (FAO, 2015) (Unit: M ha). Global/Regional forest area was calculated based on the sum of national statistics. See Supplementary Fig. 6 for the areas contained in each region.

Sub-region	1990	2000	2010
East Asia	209.20	226.82	250.50
Southeast Asia	242.05	220.97	214.59
West/Central/South Asia	116.88	118.13	124.31
Russia	808.95	809.27	815.14
Europe	185.32	193.03	198.44
Boreal North America	348.27	347.80	347.30
Temperate North America	404.23	400.76	402.98
South America	930.81	890.82	852.13
Africa	705.74	670.37	638.28
Oceania	176.83	177.64	172.00
Global	4128.27	4055.61	4015.67

Supplementary Table 5 Details of eight Dynamic Global Vegetation Models (DGVMs) used in this study. The nine models were coordinated to perform three simulations (S1, S2 and S3) following the TRENDYv2 protocol (see Methods). In simulation S1, models were forced by changing CO_2 only. In simulation S2, models were forced by changing CO_2 and climate. In simulation S3, atmospheric CO_2 concentration, climate and land use were all varied. These models were also used in the Global carbon budget 2013 (Le Quéré *et al*, 2014).

Model Name	Abbreviation	Spatial Resolution	Period	Reference
Community Land Model version 4.5	CLM4.5	1.25°×0.9375°	1860-2012	Oleson *et al.*, 2013
The Joint UK Land Environment Simulator	JULES	1.875°×1.25°	1860-2012	Clark *et al.*, 2011
Lund-Potsdam-Jena	LPJ	0.5°× 0.5°	1901-2012	Sitch *et al.*, 2003
Land Surface Processes and Exchanges	LPX	1°× 1°	1860-2012	Stocker *et al.*, 2013
ORCHIDEE-CN	OCN	1°× 1°	1860-2012	Zaehle & Friend, 2010
Organizing Carbon and Hydrology in Dynamic Ecosystems	ORCHIDEE	2°× 2°	1901-2012	Krinner *et al.*, 2005
Vegetation Integrative Simulator for Trace gases	VISIT	0.5°× 0.5°	1901-2012	Kato *et al.*, 2013
Lund-Potsdam-Jena General Ecosystem Simulator	LPJ-GUESS	0.5°× 0.5°	1901-2012	Smith *et al.*, 2001

Supplementary Table 6 Crop-specific coefficients to convert harvested biomass to carbon. The data is from Wolf *et al.* (2015) and Kyle *et al.* (2011).

Crop	Dry matter content of harvested biomass	Carbon content of harvested dry matter
Wheat	0.87	0.46
Rice (paddy)	0.91	0.46
Barley	0.87	0.46
Maize (grain)	0.86	0.46
Rye	0.9	0.46
Oats	0.87	0.46
Millet	0.89	0.46
Sorghum (grain)	0.86	0.46
Buckwheat	0.87	0.46
Quinoa	0.87	0.46
Fonio	0.89	0.46
Triticale	0.9	0.46
Canary seed	0.87	0.46
Grain, mixed	0.87	0.46
Cereals, nes	0.95	0.46
Potatoes	0.2	0.41
Sweet potatoes	0.2	0.41
Cassava	0.88	0.44
Yautia / cocoyam	0.2	0.41
Taro / cocoyam	0.2	0.41
Yams	0.2	0.41
Roots and tubers, nes	0.2	0.41
Sugar cane	0.26	0.41
Sugar beet	0.15	0.41
Beans, dry	0.84	0.46
Broad beans and horse beans, dry	0.84	0.46
Peas, dry	0.87	0.46

Chick peas	0.87	0.46
Cow peas, dry	0.84	0.46
Pigeon peas	0.87	0.46
Lentils	0.84	0.46
Bambara beans	0.91	0.46
Vetches for feed	0.35	0.44
Pulses, nes	0.3	0.46
Brazil nuts, with shell	0.8	0.6
Cashew nuts, with shell	0.8	0.6
Chestnut	0.8	0.6
Almonds, with shell	0.8	0.6
Walnuts, with shell	0.8	0.6
Pistachios	0.8	0.6
Kola nuts	0.8	0.6
Hazelnuts, with shell	0.8	0.6
Areca nuts	0.8	0.6
Nuts, nes	0.8	0.6
Soybeans	0.88	0.52
Groundnuts/peanuts (with shell)	0.91	0.6
Coconuts	0.2	0.63
Oilpalm fruit with kernel	0.65	0.62
Palm kernels	0.65	0.62
Oil, palm	0.3	0.62
Olives	0.3	0.62
Karite nuts (sheanuts)	0.8	0.6
Sunflower seed	0.91	0.62
Rapeseed	0.93	0.62
Tung nuts	0.8	0.6
Safflower seed	0.92	0.62
Sesame seed	0.95	0.62
Mustard seed	0.92	0.62
Seed cotton	0.92	0.54

Cottonseed	0.92	0.54
Linseed	0.92	0.62
Hempseed	0.91	0.62
Oilseeds nes	1	0.62
Cabbages and other brassicas	0.08	0.41
Artichokes	0.3	0.41
Asparagus	0.3	0.41
Lettuce and chicory	0.04	0.41
Spinach	0.08	0.41
Tomatoes	0.05	0.41
Cauliflowers and broccoli	0.08	0.41
Pumpkins, squash, and gourds	0.3	0.41
Cucumbers and gherkins	0.04	0.41
Eggplants (aubergines)	0.2	0.41
Chillies and peppers, green	0.09	0.41
Onions inc. Shallots, green	0.1	0.41
Onions, dry	0.1	0.41
Garlic	0.36	0.41
Leeks, other alliaceous vegetables	0.3	0.41
Beans, green	0.21	0.41
Peas, green	0.21	0.41
String beans	0.21	0.41
Carrots and turnips	0.13	0.41
Okra	0.09	0.41
Maize, green	0.2	0.44
Mushrooms and truffles	1	0.44
Vegetables, fresh nes	1	0.44

Bananas	0.26	0.41
Plantains	0.35	0.41
Oranges	0.2	0.41
Tangerines, mandarins, clementines, satsumas	0.2	0.41
Lemons and limes	0.2	0.41
Grapefruit (inc. pomelos)	0.2	0.41
Fruit, citrus nes	0.2	0.41
Apples	0.2	0.41
Pears	0.2	0.41
Quinces	0.2	0.41
Apricots	0.2	0.41
Cherries, sour	0.2	0.41
Cherries	0.2	0.41
Peaches and nectarines	0.2	0.41
Plums and sloes	0.2	0.41
Fruit, stone nes	0.2	0.41
Fruit, pome nes	0.2	0.41
Strawberries	0.08	0.41
Raspberries	0.13	0.41
Currants	0.2	0.41
Blueberries	0.15	0.41
Cranberries	0.1	0.41
Berries nes	0.1	0.41
Grapes	0.19	0.41
Watermelons	0.08	0.41
Other melons, inc. cantaloupes	0.1	0.41
Figs	0.3	0.41
Mangoes, mangosteens, guavas	0.2	0.41
Avocados	0.2	0.41
Pineapples	0.2	0.41

Dates	0.77	0.41
Persimmons	0.2	0.41
Cashewapple	0.2	0.41
Kiwi fruit	0.2	0.41
Papayas	0.2	0.41
Fruit, tropical fresh nes	0.2	0.41
Fruit, fresh nes	0.3	0.41
Coffee, green	1	0.44
Cocoa, beans	1	0.46
Tea	1	0.44
Pepper (piper spp.)	1	0.44
Chillies and peppers, dry	0.9	0.41
Vanilla	1	0.44
Cinnamon (canella)	1	0.44
Cloves	1	0.44
Nutmeg, mace and cardamoms	1	0.44
Anise, badian, fennel, coriander	1	0.44
Ginger	0.3	0.41
Spices, nes	1	0.44
Pyrethrum, dried	1	0.44
Flax fibre and tow	0.92	0.44
Hemp tow waste	0.92	0.44
Kapok fibre	0.92	0.44
Jute	0.92	0.44
Bastfibres, other	0.92	0.44
Ramie	0.92	0.44
Sisal	0.92	0.44
Agave fibres nes	0.92	0.44
Manila fibre (abaca)	0.92	0.44
Coir	0.92	0.44

Fibre crops nes	0.92	0.44
Tobacco, unmanufactured	0.8	0.44

Supplementary Table 7 Lateral carbon fluxes exported to ocean by rivers. The data is from 45 major zones (MARCATS: MARgins and CATchments Segmentation) and 149 sub-units (COSCATs: Coastal Segmentation and related CATchments). The Unit for DOC, POC and DIC is TgC yr^{-1}.

Continent	Area	MARCATs	COSCATs	DOC	POC	DIC
East Asia	China Sea and Kuroshio	39	1322	0.35	0.77	0.58
			1323	1.19	2.26	1.91
			1324	0.5	0.52	0.74
			1325	0.18	0.12	0.35
			1326	4.45	2.5	10.72
	Sea of Japan	40	1320	0.47	0.5	0.83
			1321	0.53	0.83	0.85
Southeast Asia	Tropical Eastern Indian	32	1334	0.87	1.11	1.4
			1335	4.55	7.02	14.15
	Northern Australia	37	1330	2.9	2.7	3.71
			1333	0.01	0.49	0.05
			1416	2.2	2.04	4.64
			1401	2.7	2.67	4
	South East Asia	38	1327	2.55	2.39	6.88
			1328	2.87	2.89	3.69
			1329	4.45	5.04	12.72
			1331	1.75	3.66	3.19
West/Central/ South Asia	Mediterranean Sea	20	1301	0.15	0.28	0.72
	Black Sea	21	1303	0.2	0.28	0.5
	Western Arabian Sea	27	1341	0	0.01	0
	Persian Gulf	28	1344	0	0	0
	Persian Gulf	29	1342	0.22	0.06	1.78
	Eastern Arabian Sea	30	1338	0.31	0.42	0.38
			1339	0.7	0.85	1.14
			1340	0.29	0.1	0.76
	Bay of Bengal	31	1336	7.03	17.07	9.21
			1337	1.16	1.33	1.83
Russia	Sea of Okhotsk	41	1317	0.64	0.29	0.66

			1318	1.9	1.08	2.81
			1319	0.14	0.1	0.25
			1314	0.28	0.17	0.39
	North Western Pacific	42	1315	0.2	0.13	0.38
			1316	0.25	0.26	0.35
			1309	2.46	1.88	6.75
			1310	0.16	0.13	0.16
	Siberian Shelves	43	1311	0.97	0.48	0.99
			1312	0	0	0.01
			1313	0.11	0.07	0.14
			1307	2.97	1.37	2.75
	Barent and Kara Seas	44	1308	2.94	1.22	5.47
	North Eastern Pacific	16	407	0.69	0.74	1.25
			402	0.79	0.44	1.72
	North Eastern Atlantic	17	403	1.32	0.61	3.24
			404	0.51	0.24	1.46
	Baltic Sea	18	405	0.56	0.26	0.78
			406	0.48	0.11	0.85
			401	0.52	0.34	1.95
	Iberian Upwelling	19	419	0.25	0.22	0.6
Europe			418	0.33	0.45	1.66
			416	0.54	0.88	3.3
	Mediterranean Sea	20	417	0.04	0.06	0.3
			415	0.07	0.09	0.62
			414	0.22	0.37	0.84
			412	1.22	0.53	3.93
	Black Sea	21	411	0.16	0.16	0.62
			408	1.88	0.77	3.91
	Barent and Kara Seas	44	409	0.01	0	0
			809	1.99	1.86	2.94
Boreal North	North Eastern Pacific	1	810	1.08	1.27	2.71
America			811	0.05	0.01	0.16
	Sea of Labrador	11	821	0.88	0.27	1.25

	Hudson Bay	12	822	0.1	0.09	0.14
			824	0.85	0.22	1.05
			825	3.17	0.57	6.24
			817	1.91	0.39	3.13
			818	2.12	0.28	3.19
			819	0.36	0.08	0.43
			820	0.13	0.08	0.45
	Canadian Archipelagos	13	814	0.03	0.02	0.29
			815	1.77	1.08	3.35
			816	0.21	0.56	0.61
	North Western Pacific	42	823	0.1	0.23	0.13
			812	0.64	0.25	1.43
			813	0.5	0.41	1.92
Temperate North America	Californian Current	2	804	0.13	0.14	0.16
			805	0.05	0.08	0.03
			806	0	0.01	0
	Tropical Eastern Pacific	3	807	0.24	0.23	0.25
			808	1.42	0.8	2.12
			803	0.28	0.43	0.7
			802	0.48	0.72	0.62
			801	0.23	0.35	0.34
	Caribbean Sea	8	830	1.38	1.57	1.48
			831	0.83	1.15	2.3
	Gulf of Mexico	9	832	0.83	1.02	3.91
			833	0.25	0.34	1.21
			834	4	1.99	10.27
	Florida Upwelling	10	826	0.43	0.1	0.59
			827	1.6	0.5	2.55
			828	0.78	0.39	2.09
South America	Tropical Eastern Pacific	3	1116	1.23	1.03	1.19
			1115	0.14	0.16	0.1
	Tropical Eastern Pacific	4	1112	0.39	0.38	0.82
			1113	0.04	0.37	0.09

	Southern America	5	1114	0.05	0.11	0.12
			1109	0.28	0.41	0.51
			1110	0.12	0.28	0.53
			1111	0.79	1.07	1.66
	Brazilian Current	6	1106	0.71	0.23	2.6
			1107	0.83	0.58	1.29
			1108	3.8	0.92	5.07
	Tropical Western Atlantic	7	1103	7.06	1.87	6.3
			1104	34.63	19.3	30.58
			1105	1.11	0.39	1
	Caribbean Sea	8	1102	0.26	0.37	0.3
			1101	1.57	1.61	2.14
Africa	Mediterranean Sea	20	1	0.05	0.24	0.4
			2	0	0.02	0.02
			3	0.01	0.07	0.01
	Moroccan Upwelling	22	19	0.56	0.42	0.96
			20	0	0	0
			21	0.03	0.12	0.13
	Tropical Eastern Atlantic	23	14	6.96	2.22	11.42
			15	1.73	1.76	2.56
			16	2.05	0.91	2.72
			17	0.54	0.38	0.54
			18	1.44	1.82	1.65
	Southern Western Africa	24	13	0.07	1.14	0.08
	Agulhas Current	25	9	0.71	0.66	1.06
			10	0.25	0.4	0.62
			11	1.79	0.73	3.95
	Tropical Western Indian	26	12	0.16	1.59	0.24
			7	0.88	1.45	0.89
			8	0.53	0.53	1.17
	Western Arabian Sea	27	5	0	0.14	0
			6	0.12	0.38	0.2

	Rea Sea	28	4	0.03	0.71	0.02
Oceania	Tropical Eastern Indian	32	1414	0.15	0.29	0.04
	Leeuwin Current	33	1413	0.05	0.04	0.07
	Southern Australia	34	1411	0.21	0.17	0.26
			1412	0.05	0.08	0.07
	Eastern Australian Current	35	1410	0.28	0.2	0.39
	New Zealand	36	1405	0.16	0.03	0.13
			1406	0.2	0.14	0.43
			1407	0.24	0.14	0.4
			1408	0.37	0.26	0.3
			1409	0.49	0.53	0.48
	Northern Australia	37	1403	2.62	2.05	5.9
			1402	0.64	0.76	0.89
			1415	0.95	0.64	0.76
Greenland	Northern Greenland	14	501	0.02	0.07	0
			502	0.12	0.14	0.23
			505	0.08	0.05	0.09
	Southern Greenland	15	503	0.09	0.06	0.04
			504	0.18	0.06	0.2
Antarctic	Antarctic Shelves	45	1501	0	0	0
			1502	0	0	0
			1503	0	0	0
			1504	0	0	0
			1505	0	0	0

Supplementary Fig. 1 Same as Figure 1, but using a 5-year moving window. Years on the horizontal axis in the left panel represent the central year of each moving time window.

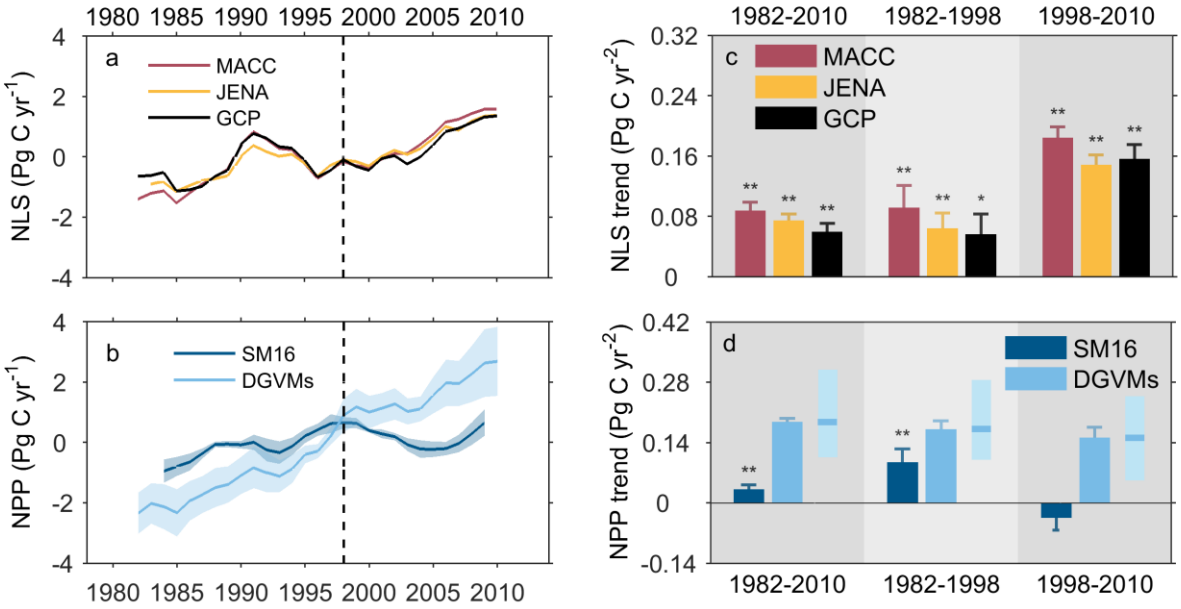

Supplementary Fig. 2 Temporal evolutions and linear trends of net land carbon sink (NLS) estimated by different versions of JENA atmospheric CO_2 inversions. The seven versions differ in number of atmospheric sites used in the inversion and the corresponding period of validity (Supplementary Table 3). In panel (b), only versions of JENA cover the whole period of 1998-2012 were used to estimate the linear trends. The errorbars indicate the uncertainty of the linear trend estimated as the standard error of linear regression coefficient (slope) (see Methods). We denote significant trends ($P < 0.05$) with two asterisk and marginally significant trends ($P < 0.1$) with one asterisk based on t test. Note that the NLS derived from all versions of JENA atmospheric inversion have been "fossil corrected" (see Methods).

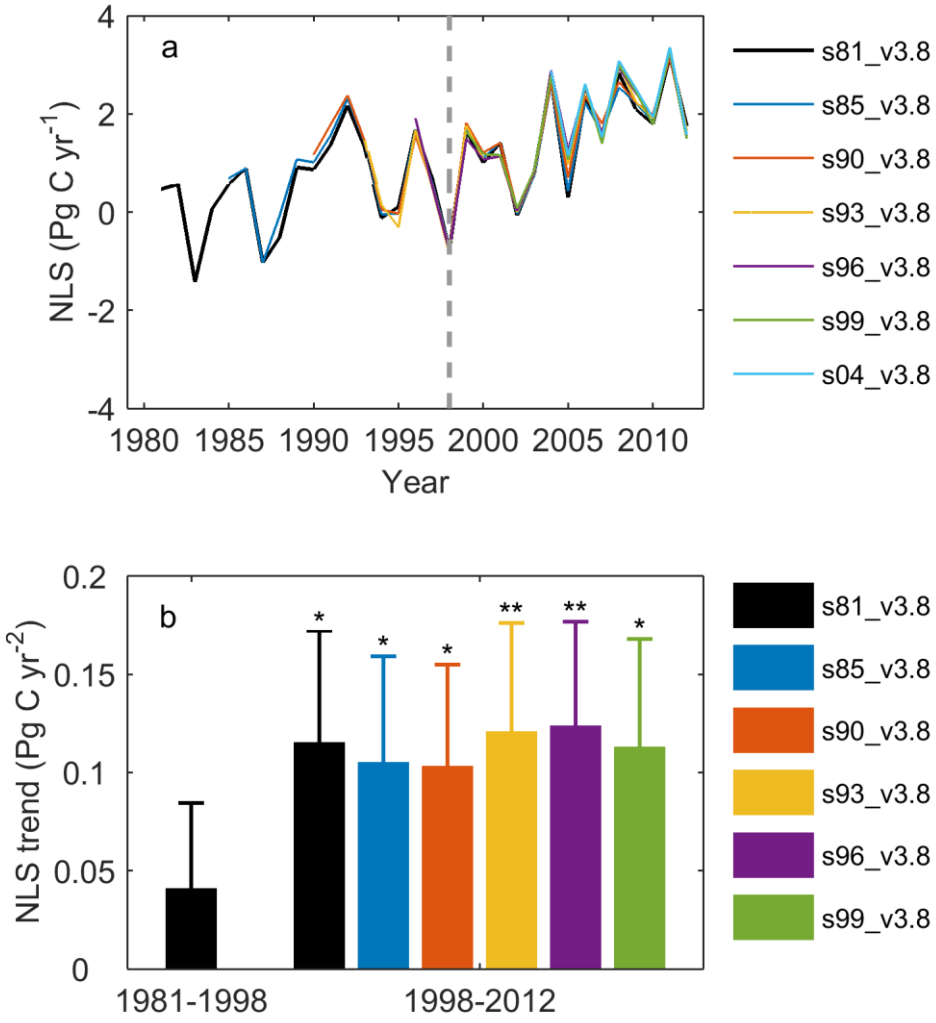

Supplementary Fig. 3 Anomalies and liner trends of global annual net primary productivity (NPP) derived from a recent study by Smith et al. (2016) (SM16) and TRENDYv2 models. Here TRENDYv2 model results driven by varying CO_2 and climate (simulation S2) are shown. In panel (b), the bars refer to the NPP trend derived from SM16 during each period and two asterisks indicate significant trends ($P < 0.05$) for GIMMS NPP based on t test. The errorbars indicate the uncertainty of the linear trend estimated as the standard error of linear regression coefficient (slope) (see Methods). For TRENDYv2 models, we donate significant trends ($P < 0.05$) with solid circles and insignificant trends ($P > 0.05$) with hollow circles. Different colors correspond to different sources of data, which are noted in the legends of each panel. In panel (c), the change in NPP trend was calculated as the difference between the NPP trend during second period (1998-2012) and that during the first period (1980-1998). The errorbars indicate data uncertainty (±1σ), which was estimated in 500 bootstrap analyses. Note that the NPP data derived from GIMMS start from 1982.

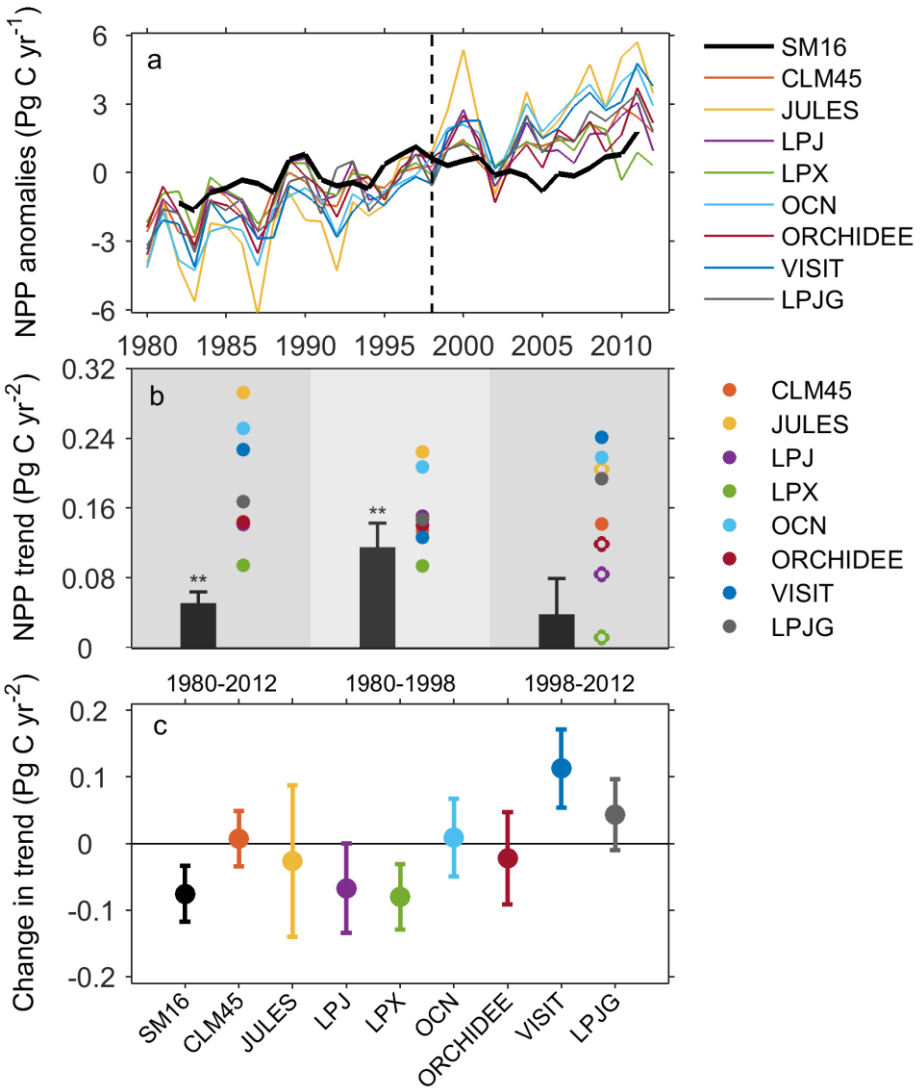

Supplementary Fig. 4 Anomalies and liner trends of global annual leaf area index (LAI) derived from GIMMS and TRENDYv2 models. Here TRENDYv2 model results driven by varying CO_2 and climate (simulation S2) are shown. In panel (b), the bars refer to the LAI trend derived from GIMMS during each period and two asterisks indicate significant trends ($P < 0.05$) for GIMMS LAI based on t test. The errorbars indicate the uncertainty of the linear trend estimated as the standard error of linear regression coefficient (slope) (see Methods). For TRENDYv2 models, we donate significant trends ($P < 0.05$) with solid circles and insignificant trends ($P > 0.05$) with hollow circles. Different colors correspond to different sources of data, which are noted in the legends of each panel. In panel (c), the change in LAI trend was calculated as the difference between the LAI trend during second period (1998-2012) and that during the first period (1980-1998). The errorbars indicate data uncertainty (±1σ), which was estimated in 500 bootstrap analyses. Note that the LAI data derived from GIMMS start from 1982.

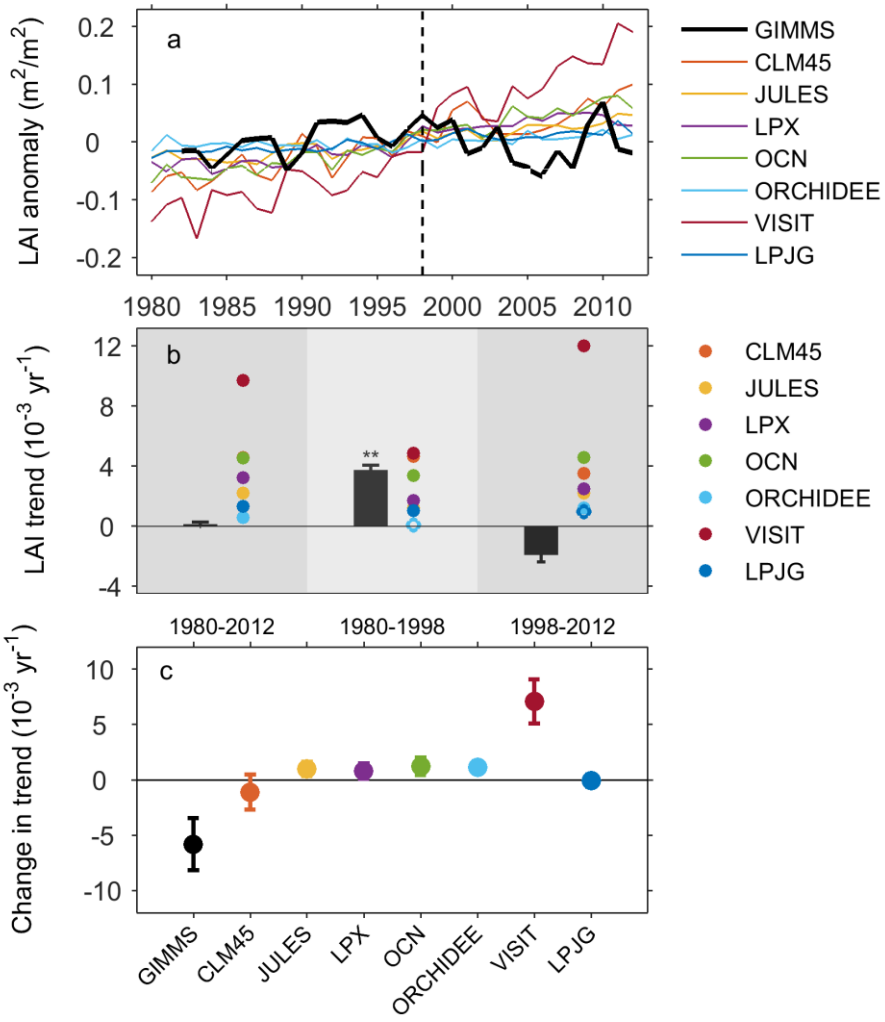

Supplementary Fig. 5 Anomalies and liner trends of fire emissions. In panel (a), results from the Reanalysis of the Troposphere chemical composition (RETRO) project and satellite-derived product (GFED) are shown. In panel (b), results from four DGVMs are shown. Note that RETRO dataset is only available from 1960 to 2000, and GFED dataset is only available since 1997. We denote significant trends ($P < 0.05$) with two asterisk and marginally significant trends ($P < 0.1$) with one asterisk based on t test. The errorbars indicate the uncertainty of the linear trend estimated as the standard error of linear regression coefficient (slope) (see Methods).

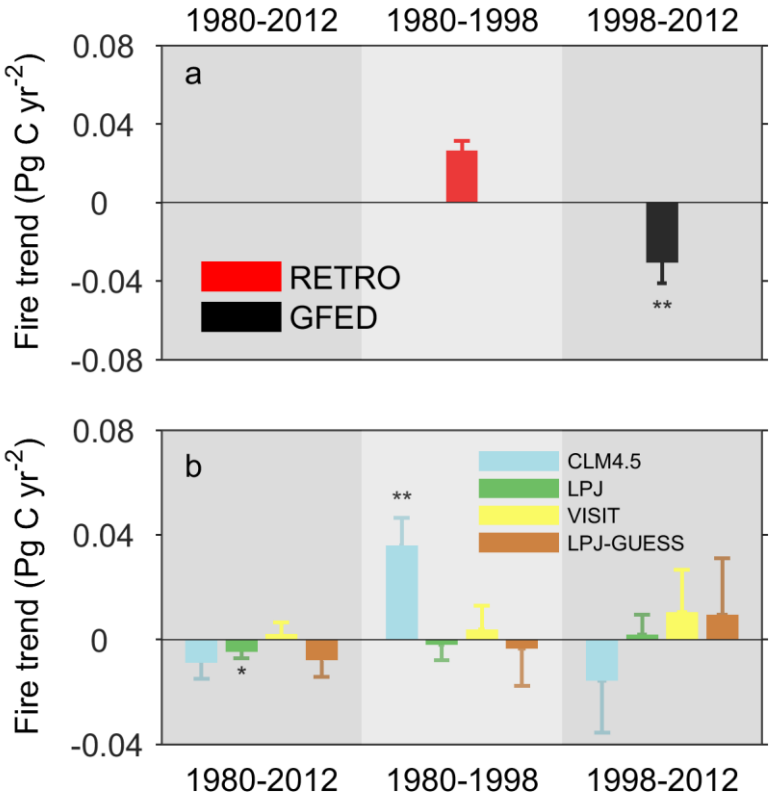

Supplementary Fig. 6 Change in forest area during 1990-2010, 1990-2000 and 2000-2010 by sub-region (Unit: M ha yr^{-1}) derived from the Forest Resources Assessment 2015 by Food and Agriculture Organization of the United Nations (FAO, 2015). Here we divided the world into ten regions: East Asia, Southeast Asia, West/Central/South Asia, Russia, Europe, Boreal North America, Temperate North America, South America, Africa and Oceania. Colored bars in the upward direction indicates an increase in forest area during the period, whereas bars in the downward direction indicates a decrease in forest area. Note that the change in forest area during 1990-2010, 1990-2000 and 2000-2010 are marked in gray, red and green, respectively. The detailed information on forest area can be found in Supplementary Table 4.

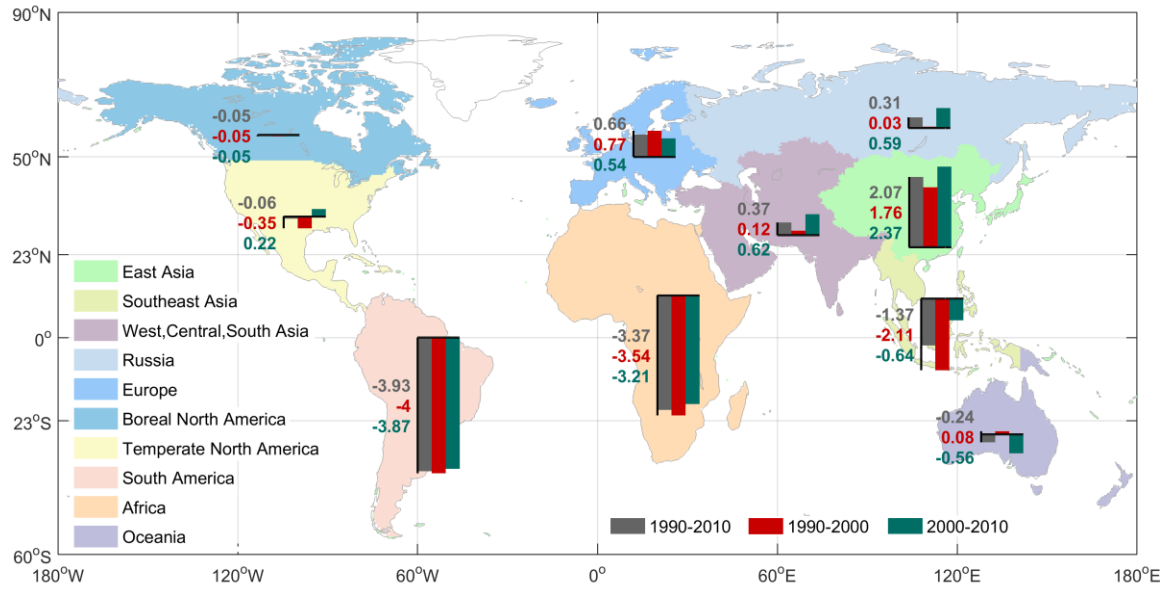

Supplementary Fig. 7 Average net carbon emission from land use change (E_{LUC}) during 1980-2012 (a) and change in E_{LUC} trend between 1998-2012 and 1980-1998 (b). The bottom left of (a) and (b) show the results at latitudinal scale, including boreal (50°N-90°N), northern temperate (23°N-50°N), tropiccal (23°N-23°S) and southern temperate region (23°S-60°S). E_{LUC} during 1980-2012 and change in E_{LUC} trend between two periods are obtained based on five approaches: two bookkeeping methods ($BK_{Houghton}$ and BK_{Hansis}; see Methods), an inversion-DGVMs combination method ($E_{Inversion\text{-}LF\text{-}DGVMs(S2)}$; see Methods), and also estimates based on DGVMs from TRENDYv2 and TRENDYv4 project. The DGVMs approach calculated carbon emissions from land use change (E_{LUC}) by using the difference of net land-atmosphere fluxes between simulation S3 and simulation S2. In simulation S2, atmospheric CO_2 and climate were varied. In simulation S3, atmospheric CO_2, climate and land use were varied. In panel (b), a positive trend refers to increased E_{LUC} during corresponding period, while a negative trend refers to decreased E_{LUC} during corresponding period. The errorbars in panel (b) indicate data uncertainty (±1σ), which was estimated in 500 bootstrap analyses.

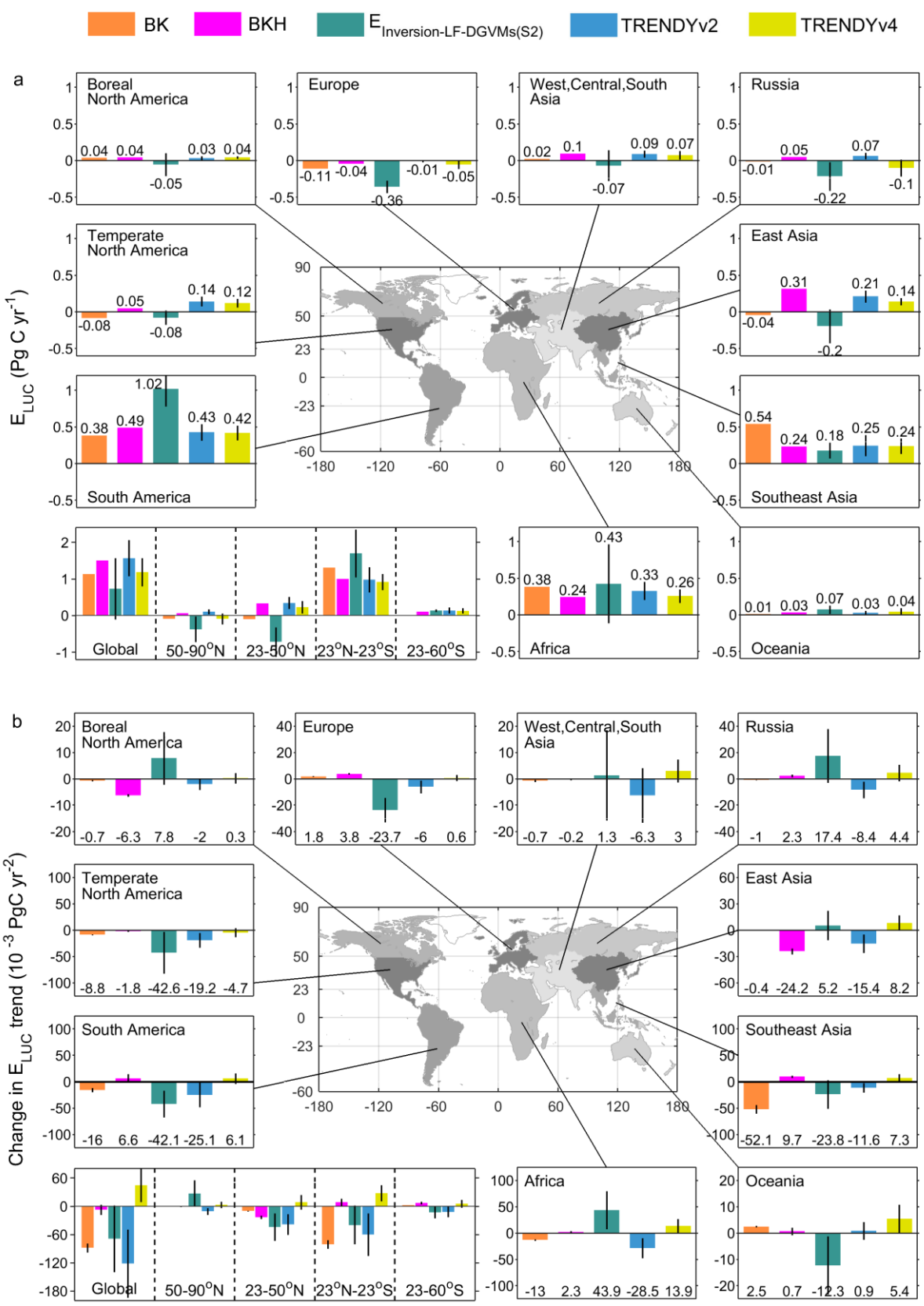
BK
BKH
E Inversion-LF-DGVMs(S2)
TRENDYv2
TRENDYv4
a
E LUC (Pg C yr-1)
Boreal North America
0.04 0.04 -0.05 0.03 0.04
Europe
-0.11 -0.04 -0.36 -0.01 -0.05
West,Central,South Asia
0.02 0.1 -0.07 0.09 0.07
Russia
-0.01 0.05 -0.22 0.07 -0.1
Temperate North America
-0.08 0.05 -0.08 0.14 0.12
East Asia
-0.04 0.31 -0.2 0.21 0.14
South America
0.38 0.49 1.02 0.43 0.42
Southeast Asia
0.54 0.24 0.18 0.25 0.24
Global
50-90°N
23-50°N
23°N-23°S
23-60°S
Africa
0.38 0.24 0.43 0.33 0.26
Oceania
0.01 0.03 0.07 0.03 0.04
b
Change in E LUC trend (10 -3 PgC yr-2)
Boreal North America
-0.7 -6.3 7.8 -2 0.3
Europe
1.8 3.8 -23.7 -6 0.6
West,Central,South Asia
-0.7 -0.2 1.3 -6.3 3
Russia
-1 2.3 17.4 -8.4 4.4
Temperate North America
-8.8 -1.8 -42.6 -19.2 -4.7
East Asia
-0.4 -24.2 5.2 -15.4 8.2
South America
-16 6.6 -42.1 -25.1 6.1
Southeast Asia
-52.1 9.7 -23.8 -11.6 7.3
Global
50-90°N
23-50°N
23°N-23°S
23-60°S
Africa
-13 2.3 43.9 -28.5 13.9
Oceania
2.5 0.7 -12.3 0.9 5.4

Supplementary Fig. 8 Change in forest area during 1990-2015 in China (Unit: M ha) derived from Land Use Harmonization (LUH) data and that from forest inventory data.

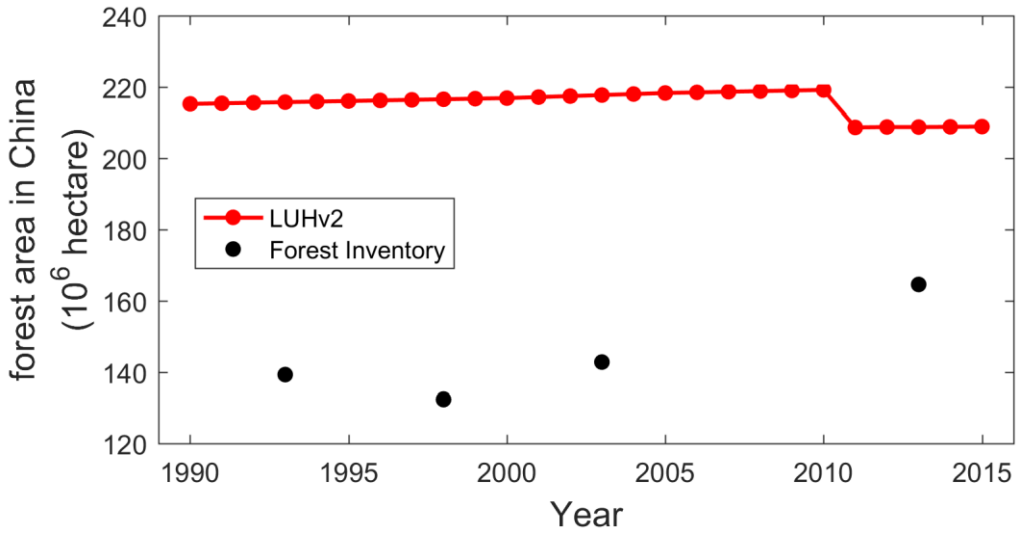

Supplementary Fig. 9 Anomalies of satellite-derived net primary productivity (NPP) during 1980-2012. Anomalies are obtained by removing from each year the mean over 1980-2012. The satellite-derived NPP is from MODIS C5 and a recent study by Smith *et al.* (SM16), respectively. The shaded area in the left panels indicates data uncertainty (±1σ).

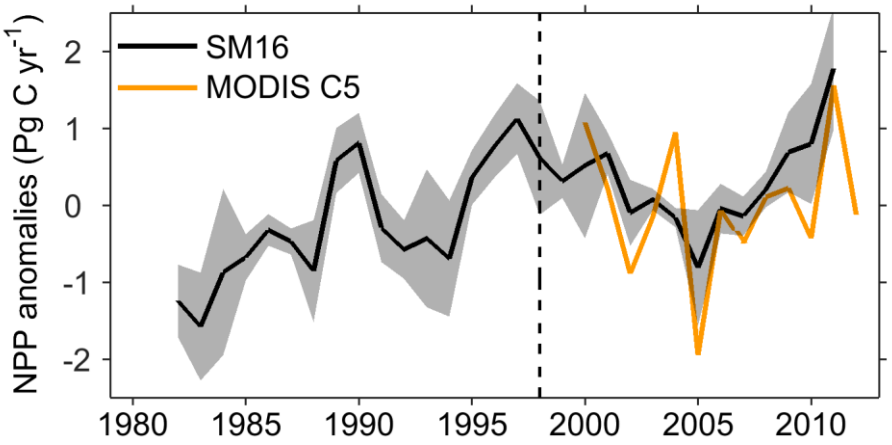

Supplementary Fig. 10 Liner trends of global annual net land carbon sink (NLS) with two different TRENDY versions (TRENDYv2 and TRENDY v4) under different scenarios considered. In simulation S2, atmospheric CO_2 and climate were varied. In simulation S3, atmospheric CO_2, climate and land use were varied. Note that only models included in both TRENDYv2 and TRENDYv4 are used in comparison. In panel (a) to (g), we denote significant trends ($P < 0.05$) with two asterisk and marginally significant trends ($P < 0.1$) with one asterisk based on t test. The errorbars indicate the uncertainty of the linear trend estimated as the standard error of linear regression coefficient (slope) (see Methods). In panel (h), NLS trends estimated by different models in each version and under each scenario were averaged, with the errorbar representing the uncertainty of the linear trend (see Methods). A positive trend refers to increased E_{LUC} during corresponding period, while a negative trend refers to decreased E_{LUC} during corresponding period.

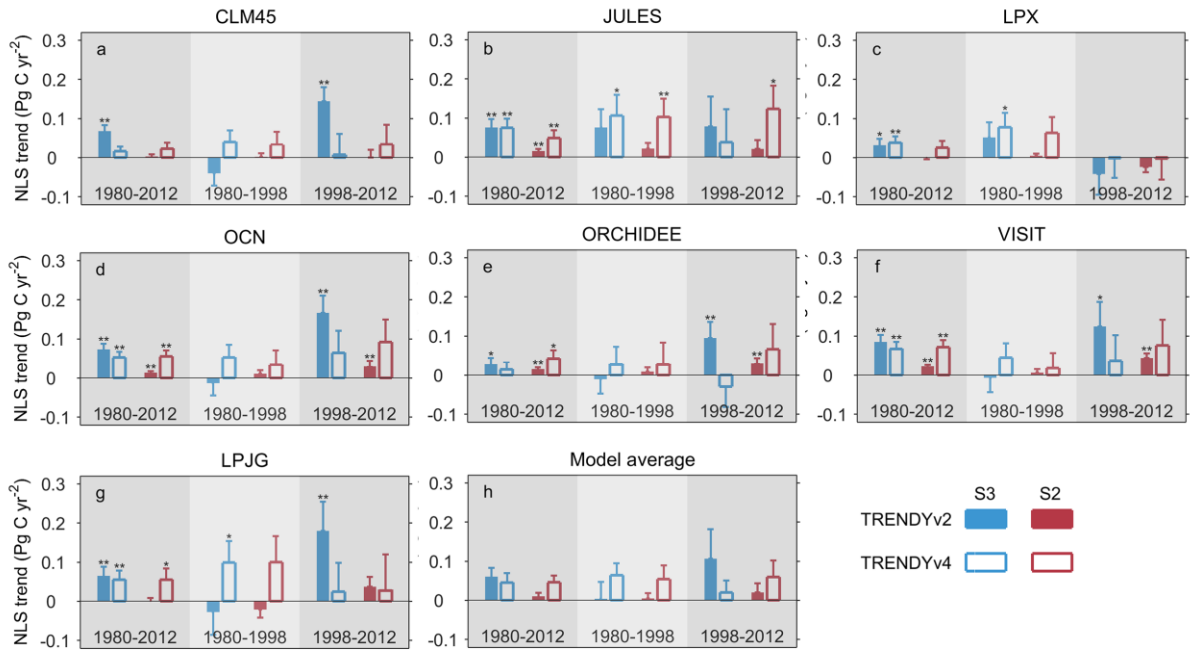

Supplementary Fig. 11 Comparison of the global annual fossil fuel and cement production emissions (PgC yr^{-1}) used in Global Carbon Project (GCP) and two atmospheric inversions.

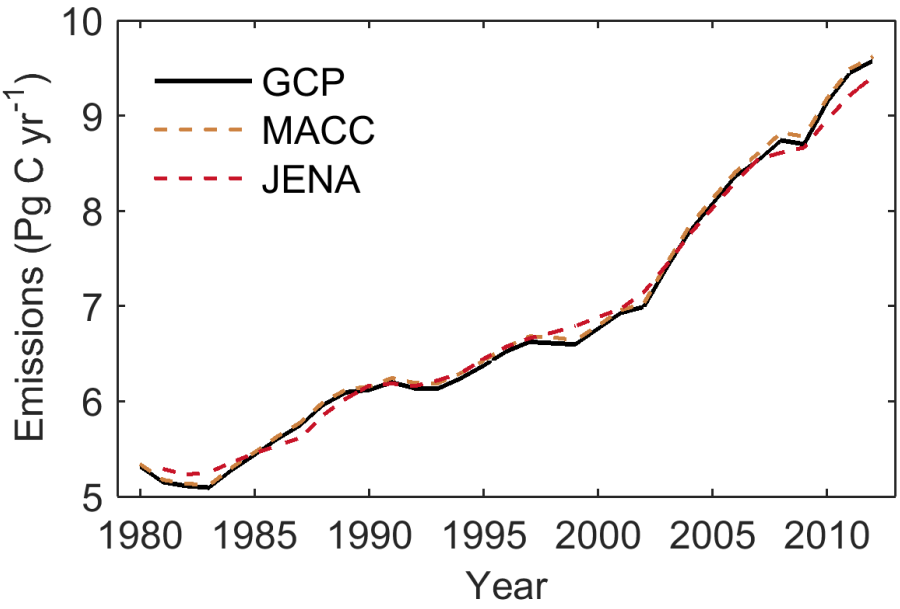

Supplementary Fig. 12 Average carbon flux associated with crop (red) and wood (green) trade during 1980-2012 (a) and change in its trend between 1998-2012 and 1980-1998 (b). The results of net trade (import - export) are shown. In panel (a), a positive value indicates a net import of crop/wood, whereas a negative value indicates a net export of crop/wood. In panel (b), a positive value indicates an increasing net import or a decreasing net export during 1998-2010 compared with 1980-1998. Note that 1 Tg C = 10^{-3} Pg C.

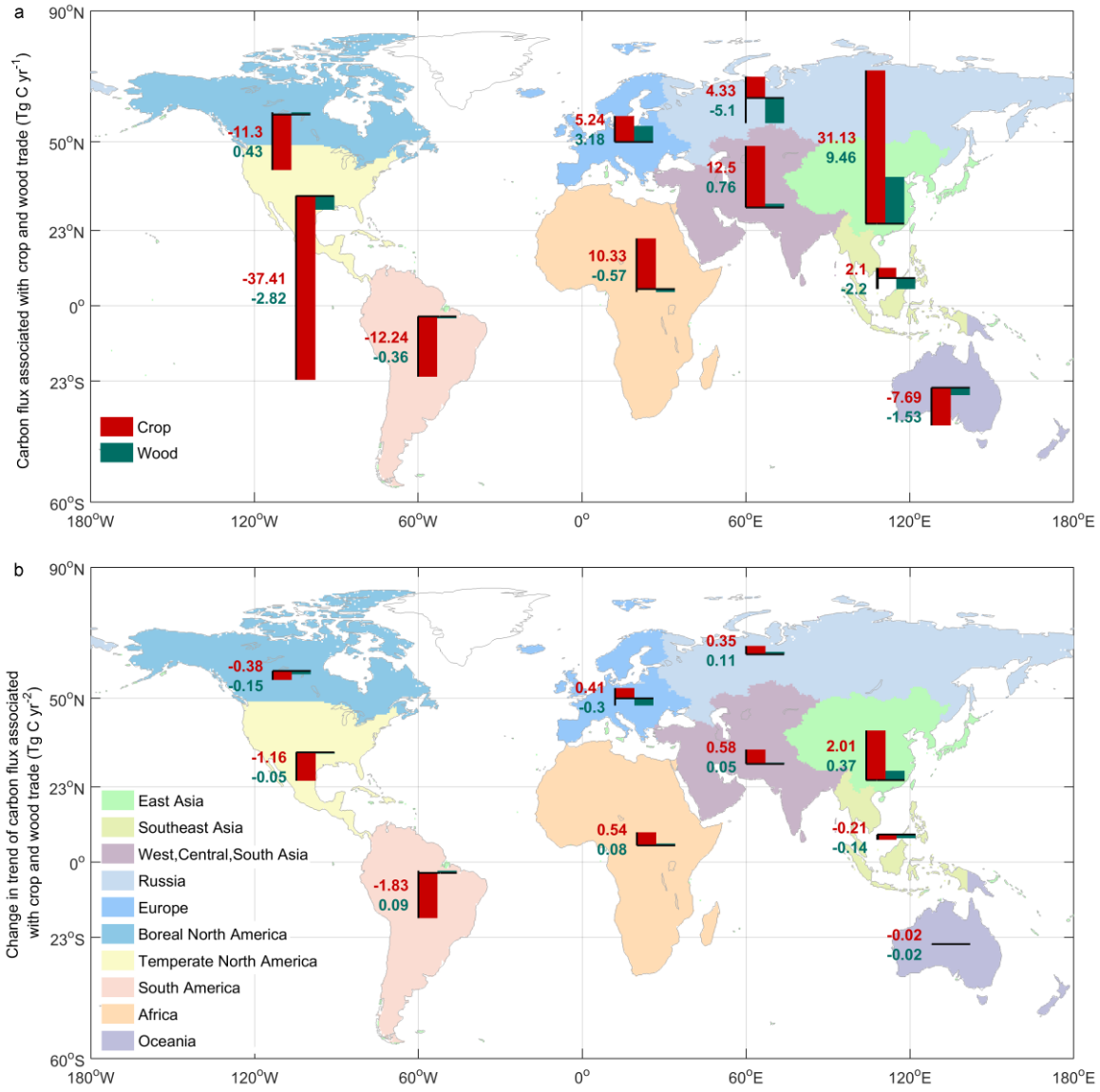

Supplementary Fig. 13 The transport of carbon (DOC, POC and DIC) to ocean by sub-region (Unit: Tg C yr^{-1}). The detailed information for each major zone (MARCATS: MARgins and CATchments Segmentation) and sub-units (COSCATs: Coastal Segmentation and related CATchments) can be found in Supplementary Table 7.

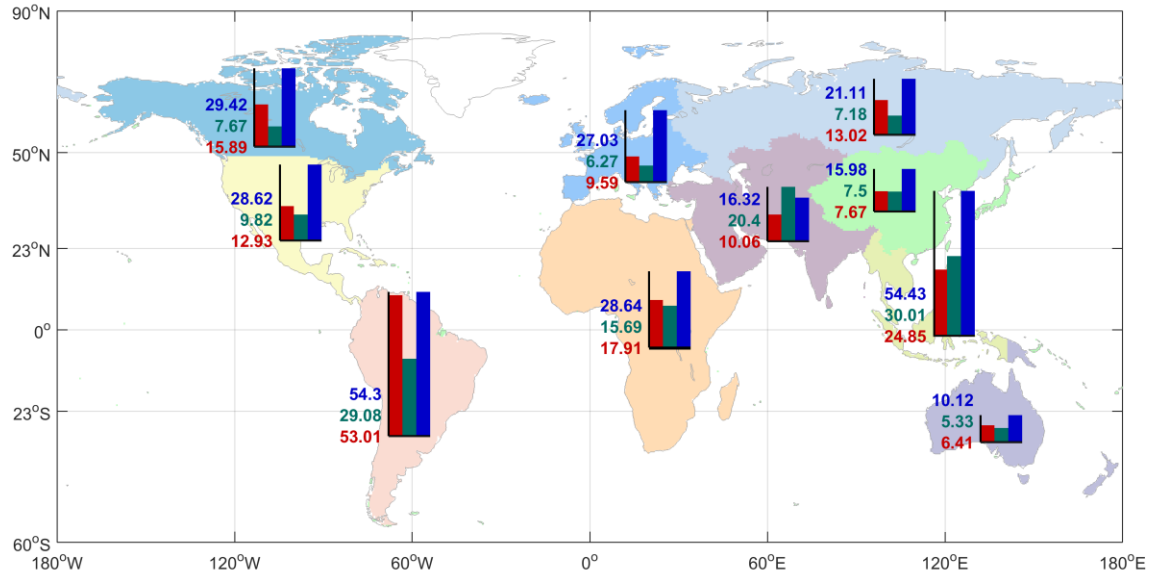

Supplementary Fig. 14 Average net carbon emission from land use change (E_{LUC}) during 1980-2012 (a) and change in E_{LUC} trend between 1998-2012 and 1980-1998 (b). The bottom left of (a) and (b) show the results at latitudinal scale, including boreal (50^oN-90^oN), northern temperate (23^oN-50^oN), tropical (23^oN-23^oS) and southern temperate region (23^oS-60^oS). E_{LUC} during 1980-2012 and change in E_{LUC} trend between two periods are obtained based the inversion-DGVMs combination method ($E_{Inversion\text{-}LF\text{-}DGVMs(S2)}$; including results with all data resampled into a common $0.5^o \times 0.5^o$, $1^o \times 1^o$ or $2^o \times 2^o$ grid). In panel (b), a positive trend refers to increased E_{LUC} during corresponding period, while a negative trend refers to decreased E_{LUC} during corresponding period.

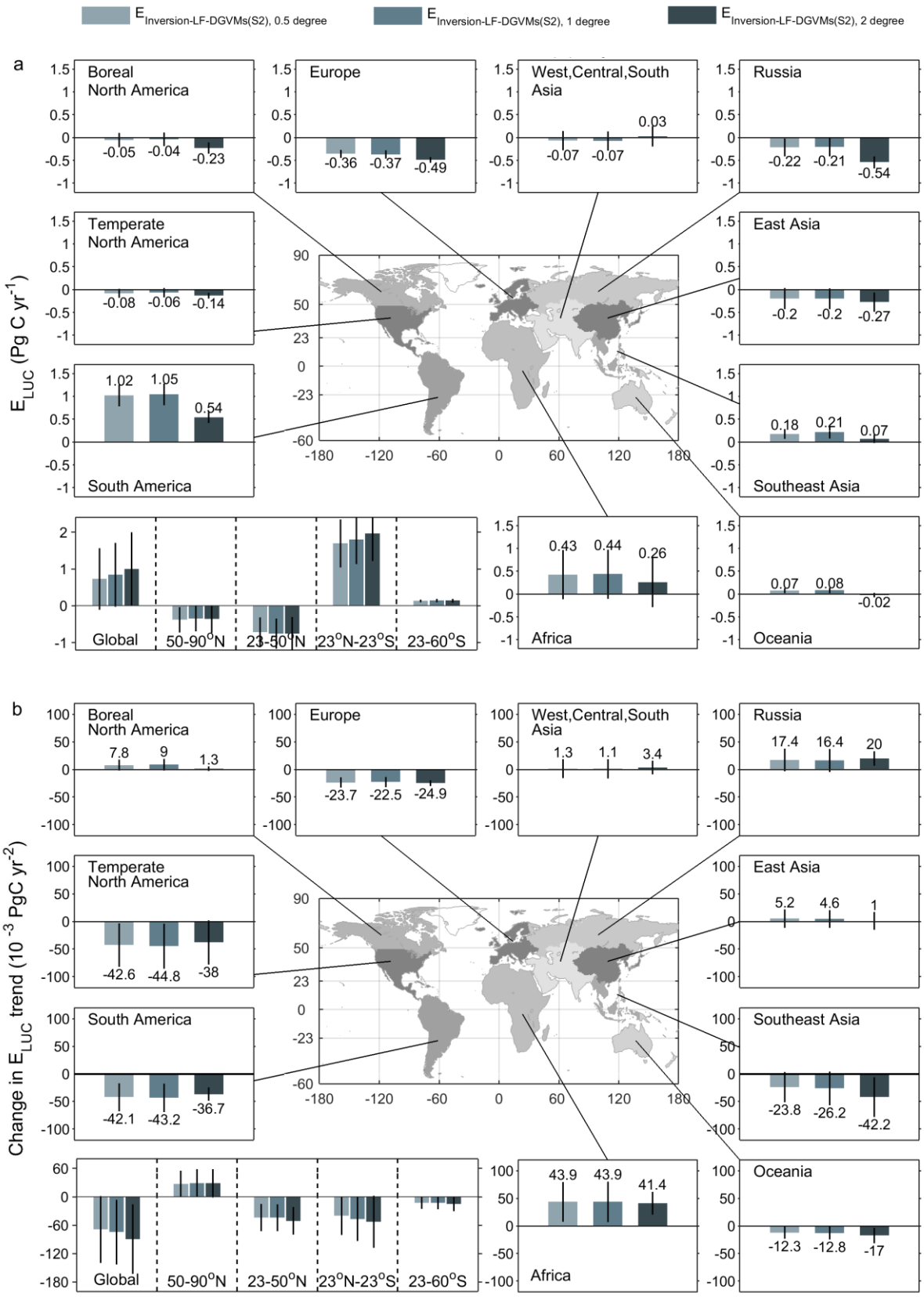
E Inversion-LF-DGVMs(S2), 0.5 degree
E Inversion-LF-DGVMs(S2), 1 degree
E Inversion-LF-DGVMs(S2), 2 degree
a
E_LUC (Pg C yr-1)
Boreal North America
-0.05 -0.04 -0.23
Europe
-0.36 -0.37 -0.49
West,Central,South Asia
-0.07 -0.07 0.03
Russia
-0.22 -0.21 -0.54
Temperate North America
-0.08 -0.06 -0.14
East Asia
-0.2 -0.2 -0.27
1.02 1.05 0.54
South America
0.18 0.21 0.07
Southeast Asia
Global
50-90°N
23-50°N
23°N-23°S
23-60°S
0.43 0.44 0.26
Africa
0.07 0.08 -0.02
Oceania
b
Change in E_LUC trend (10-3 PgC yr-2)
Boreal North America
7.8 9 1.3
Europe
-23.7 -22.5 -24.9
West,Central,South Asia
1.3 1.1 3.4
Russia
17.4 16.4 20
Temperate North America
-42.6 -44.8 -38
East Asia
5.2 4.6 1
South America
-42.1 -43.2 -36.7
Southeast Asia
-23.8 -26.2 -42.2
Global
50-90°N
23-50°N
23°N-23°S
23-60°S
43.9 43.9 41.4
Africa
Oceania
-12.3 -12.8 -17

References

Clark, D.B., Mercado, L.M., Sitch, S., Jones, C.D. (2011) The Joint UK Land Environment Simulator (JULES), Model description-Part 2: Carbon fluxes and vegetation. *Geoscientific Model Development Discussions* **4**, 701-722.

Kato E., Kinoshita T., Ito A., Kawamiya M., Yamagata Y. (2013) Evaluation of spatially explicit emission scenario of land-use change and biomass burning using a process-based biogeochemical model. *Journal of Land Use Science* **8**, 104-122.

Houghton, R.A., Nassikas, A.A. (2017) Global and Regional Fluxes of Carbon from Land Use and Land-Cover Change 1850-2015. *Global Biogeochemical Cycles* **31**, doi:10.1002/2016GB005546.

Krinner, G., Viovy, N., Noblet-Ducoudré, N.D., Ogée, J., Polcher, J., Friedlingstein, P., Ciais, P., Sitch, S., Prentice, I.C. (2005) A dynamic global vegetation model for studies of the coupled atmosphere-biosphere system. *Global Biogeochemical Cycles* 19, doi:10.1029/2003GB002199.

Kyle, G.P., Luckow, P., Calvin, K.V., Emanuel, W.R., Nathan, M., Zhou, Y. (2011) GCAM 3.0 Agriculture and Land Use: Data Sources and Methods. *Office of Scientific & Technical Information Technical Reports*.

Oleson, K.W., Lawrence, D.M., Bonan, G.B. (2013) Technical description of version 4.5 of the Community Land Model (CLM). Ncar Tech. Note NCAR/TN-503+STR. National Center for Atmospheric Research, Boulder. *Geophysical Research Letters* **37**, 256-265.

Le Quéré, C., Peters, G.P., Andres, R.J., Andrew, R.M., Boden, T.A., Ciais, P., Friedlingstein, P., Houghton, R.A., Marland, G., Moriarty, R. (2014) Global carbon budget 2013. *Earth System Science Data Discussions* **7**, 521-610.

Sitch, S., Smith, B., Prentice, I.C., Arneth, A., Bondeau, A., Cramer, W., Kaplan, J.O., Levis, S., Lucht, W., Sykes, M.T. (2003) Evaluation of ecosystem dynamics, plant geography and terrestrial carbon cycling in the LPJ dynamic global vegetation model. *Global Change Biology* **9**, 161-185.

Smith, B., Prentice, I.C., Sykes, M.T. (2001) Representation of Vegetation Dynamics in the Modelling of Terrestrial Ecosystems: Comparing Two Contrasting Approaches within European Climate Space. *Global Ecology & Biogeography* **10**, 621–637.

Smith, W.K., Reed, S.C., Cleveland, C.C., Ballantyne, A.P., Anderegg, W.R.L., Wieder, W.R., Liu, Y.Y., Running, S.W. (2016) Large divergence of satellite and Earth system model estimates of global terrestrial CO_2 fertilization. *Nature Climate Change* **6**, doi:10.1038/nclimate2879.

Stocker, B.D., Roth, R., Joos, F., Spahni, R., Steinacher, M., Zaehle, S., Bouwman, L., Prentice, I.C. (2013) Multiple greenhouse-gas feedbacks from the land biosphere under future climate change scenarios. *Nature Climate Change* **3**, 2747.

Wolf, J., West, T.O., Page, Y.L., Kyle, G.P., Zhang, X., Collatz, G.J., Imhoff, M.L. (2016) Biogenic carbon fluxes from global agricultural production and consumption. *Global Biogeochemical Cycles* **29**, 1617-1639.

Zaehle, S., Friend, A.D. (2010) Carbon and nitrogen cycle dynamics in the O-CN land surface model: 1. Model description, site ‐ cale evaluation, and sensitivity to parameter estimates. *Global Biogeochemical Cycles* **24**, doi:10.1029/2009GB003521.